

Unrelaxed vacancy formation energies in group-IV elements calculated by the full-potential linear muffin-tin orbital method: Invariance with crystal structure

O. Le Bacq and F. Willaime

Section de Recherches de Métallurgie Physique, CEA/Saclay, 91191 Gif-sur-Yvette, France

A. Pasturel

Laboratoire de Physique Numérique des Systèmes Complexes, Maison des Magistères, CNRS BP 166, 38042 Grenoble, France

(Received 10 November 1998)

The unrelaxed vacancy formation energies have been calculated for group-IV elements (Ti, Zr, Hf) in the hexagonal close packed (hcp) and body centered cubic (bcc) structures within the local density approximation to the density functional theory using the full-potential linear muffin-tin orbital method. In hcp-Hf the calculated value of 2.37 eV is in excellent agreement with the experimental value of 2.45 ± 0.2 eV. The results found in hcp-Ti and hcp-Zr, i.e., 2.14 eV and 2.07 eV, respectively, can therefore be considered as reliable predictions. In the more open bcc structure, after very conclusive validations of the present procedure in Mo and W by comparison with experiments and other *ab initio* calculations, vacancy formation energies of 2.2–2.4 eV are obtained in Ti, Zr, and Hf. These energies, which are very similar to those in the hcp structure, are significantly larger than the experimental activation energies for self-diffusion in the bcc structure. Assuming that the monovacancy mechanism is dominant in β -Ti, β -Zr, and β -Hf, this demonstrates that structural relaxations with particularly large amplitudes are expected around the vacancy. [S0163-1829(99)00313-6]

I. INTRODUCTION

Group-IV elements (Ti, Zr and Hf) are known to exhibit very similar self-diffusion behaviors characterized by a strong crystal-structure dependence between the α -phase, i.e., the low temperature hexagonal close packed (hcp) structure, and the β -phase, i.e., the high temperature body-centered cubic (bcc) structure.¹ When plotted on a normalized Arrhenius plot, the self-diffusion coefficients are indeed almost identical for the three elements in a given structure, and change by several orders of magnitude from one structure to the other at the transition temperature (see Fig. 1). The intrinsic self-diffusion coefficient measurements can now be considered as reliable for these three elements in both phases, after the important improvements made recently,^{2,3} but very little is known about their defect parameters, such as defect formation and migration enthalpies.⁴

The vacancy mechanism is confirmed to be dominant in face centered cubic (fcc) metals at low temperatures; it is therefore expected to be also the case in hcp-metals, because of the strong similarities between these two structures. As a matter of fact, there is compelling evidence that intrinsic self-diffusion in α -Ti, α -Zr and α -Hf, characterized by activation energies, Q , respectively of 3.14 eV, 3.17 eV, and 3.72 eV, is normal and vacancy controlled.^{2,3,5} This mechanism is supported by the value of the vacancy formation energy, i.e., 2.45 ± 0.2 eV, which was deduced from positron annihilation spectroscopy measurements of the vacancy concentrations in α -Hf.⁶ Such studies are not possible in Ti and Zr due to the limited temperature range available for the α -phase. The determination of vacancy formation and migration enthalpies, H_f and H_m , are therefore needed in these elements to validate and characterize the vacancy mechanism. The situation is more complex in the bcc structure,

where the self-diffusion is commonly regarded as anomalous in these elements, because the activation energies—deduced from the slopes of the Arrhenius plot of the self-diffusion coefficients—normalized to the melting temperatures are two-to-three times lower than expected for *normal* diffusion, and the self-diffusion coefficients when extrapolated to half the melting temperature are more than five orders of magnitude larger than in other bcc transition metals.⁷ Several models have been proposed in the past to interpret the very wide

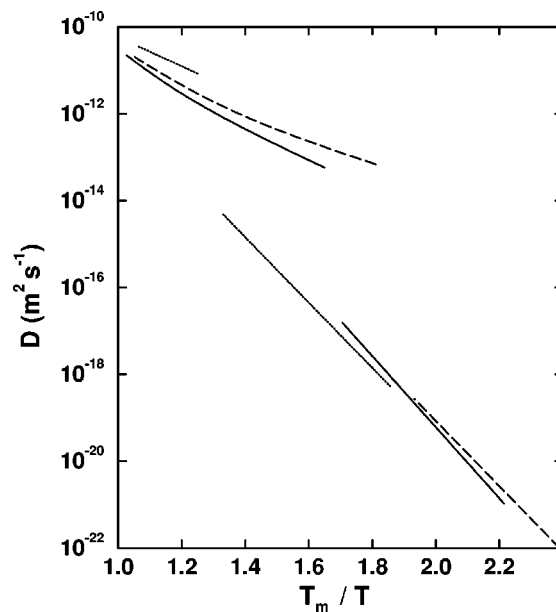


FIG. 1. Arrhenius plot for the experimental tracer self-diffusion coefficients for group IV elements in their low temperature hcp structure and high temperature bcc structure: Ti (full line), Zr (dashed line), and Hf (dotted line). The inverse temperature is normalized to the melting temperature, T_m .

spreading of self-diffusion behaviors among the various elements.⁷ Diffusion via monovacancies remains the most likely mechanism. In this context any information about their defect parameters may give the key to understand their unusual diffusion behavior. For the vacancy mechanism to be dominant in both structures, a large difference between the two structures in vacancy diffusion, i.e., in vacancy migration energy, is not sufficient, and a large difference in vacancy concentration, i.e., vacancy formation energy, is required.

The studies of defect properties with empirical potentials are not very conclusive in these elements. When based on pair potentials their predictive character is uncertain,⁸ and when more realistic many-body potentials—EAM or second moment approximation (SMA) type—are used, they suffer from the fact that the vacancy formation energy is most often one of the fitted quantity. The experimental values which were taken for the latter are now known to be incorrect. However one study, which does not have this drawback, performed in zirconium, shows that the unrelaxed vacancy formation energies are almost identical in both structures (2.14 eV and 2.10 eV in the hcp and bcc structures, respectively) and that the relaxation energy is particularly large in the bcc structure, with a value of 0.67 eV.⁹ One can now take advantage of first principles electronic structure calculations, which have recently shown to be very efficient for quantitative defect studies, to provide new data for understanding self-diffusion in these elements. The vacancy formation energies have indeed been successfully calculated within the local-density approximation to the density functional theory, in metals with cubic structure like aluminum,¹⁰ lithium,¹¹ sodium,¹² and a series of transition metals.^{13–17} The purpose of the present paper is to perform similar calculations in Ti, Zr, and Hf, both in the hcp and the bcc structures. The very specific self-diffusion behavior common to these three elements is indeed believed to originate from their similar electronic structure, as is the case for their phase diagrams. The full-potential linear muffin-tin orbital (FP-LMTO) method¹⁸ has been adopted here because (i) it allows to handle large supercells (up to 54 atoms in the present study) at a reasonable computational cost and (ii) to treat equally metals of the $3d$, $4d$ and $5d$ series making possible a systematic in group IV; and (iii) it avoids the difficulty of the generation of pseudopotentials. Because it is not possible to calculate forces within the present implementation of the FP-LMTO method, the structural relaxations around the vacancy are not taken into account in this work. The aim of the present calculations is therefore to look whether there is an intrinsic effect of the crystal structure on the unrelaxed vacancy formation energy, and to provide reference *ab initio* data for these energies in both structures. In the hcp structure the relaxation effects are expected to be small, making the calculated vacancy formation energies highly predictive, while the relaxation effects in the bcc structure are a quite open issue.

The organization of the present paper is as follows. The main characteristics of the present FP-LMTO calculations and the computational procedure are described in Sec. II. They are then validated in Sec. III by comparing with experiments and other *ab initio* calculations the vacancy formation energies in reference systems, namely Cu, Mo, and W. The

results concerning the vacancy-formation energies and volumes in the hcp and bcc structures of group-IV elements are presented and discussed in Sec. IV.

II. TECHNIQUES AND DEFINITIONS

The electronic states and the total energies presented here are calculated using the density-functional theory (DFT) within the local density approximation (LDA).^{21–23} The Kohn-Sham equations are solved using a fast full potential version of the LMTO method²⁴ proposed by Methfessel,¹⁸ which has been described in Refs. 18–20,25. Within this scheme the potential and charge density are treated without spherical-shape approximation inside the nonoverlapping muffin-tin spheres, and they are obtained by an interpolation technique in the interstitial region. In the present calculations, three LMTO envelopes of Hankel functions with kinetic energies -0.01 Ry, -1.0 Ry, and -2.3 Ry were used. For all elements, the wave-function basis set consisted of s , p , and d orbitals from the first and second envelopes, and s and p orbitals from the third envelope. For Hf, the f orbitals were added in the first and second envelopes and the d orbitals were added in the third one. Hankel functions with kinetic energies of -1 Ry and -3 Ry were used for the interstitial fit and the density and potential were expanded in spherical harmonics up to angular momentum $l_{\max}=4$ inside the spheres. The extended $3p$ (respectively $4p$ and $5p$) states of $3d$ (respectively $4d$ and $5d$) metals were treated as a semicore by performing a separate diagonalization at each iteration according to the two panel treatment.²⁵ All calculations are performed in the scalar relativistic approximation. The number of k points, n_k , used in the Brillouin zone integration will be specified in the text for the various calculations. They are taken on normal meshes, except for the calculations with 54 atomic sites, where 10 special points were used.²⁶ The k -point meshes used for the second panel are taken here to be approximately eight times less dense than for the first panel. Standard values are taken for the radii of the muffin-tin spheres, i.e., 0.84, 0.88 and 0.876 times the Wigner-Seitz radius respectively for the bcc, fcc, and hcp structures. The empty spheres used for the vacancy calculations are identical. The summation over eigenstates is performed using the Hermit-Gaussian smearing technique,²⁷ with a smearing width $\sigma=20$ mRy.

The equilibrium volumes, Ω_0 , and bulk moduli, B , are obtained by fitting Birch-Murnaghan's equation of states using 195 k points in the irreducible part of the Brillouin zone (BZ) for bcc and fcc structures, and 270 k points for the hcp structure. They are summarized in Table I, together with the c/a ratios for the hcp structure. Their agreements with experiments^{28,29} are as expected within LDA, i.e., Ω_0 and B are respectively slightly underestimated and overestimated. The comparison with previous FP-LMTO calculations in group IV shows some small scatter due to differences in the basis set for hcp-Ti and hcp-Zr (Ref. 30) and in the implementation of the FP-LMTO method for hcp-Hf.³¹ Finally, the bulk properties from the previous vacancy studies, which will be discussed in the following, are also reported in Table I for comparison, namely the FP-LMTO calculations in Mo, W, and Cu (Ref. 15) and the pseudopotential calculations in Mo (Ref. 16) and W.¹⁷

TABLE I. Calculated and experimental equilibrium volume Ω_0 , bulk moduli B , and c/a ratios for the six metals studied in their equilibrium structures, as well as in the bcc structure for group IV elements. The present FP-LMTO results are compared with other similar FP-LMTO computations as well as with the pseudopotential (PP) values for previous vacancy studies. All calculations are within LDA. Experimental data for Ω_0 and c/a are taken at room temperature from Ref. 28, while those for B are at low temperature from Ref. 29. The volumes are expressed in \AA^3 and the bulk moduli in Mbar.

		hcp-Ti	bcc-Ti	hcp-Zr	bcc-Zr	hcp-Hf	bcc-Hf	Mo	W	Cu
Ω_0	present work	16.20	15.88	21.93	21.01	21.14	20.82	15.14	15.53	10.99
	FP-LMTO	15.75 ^a		21.85 ^a		20.10 ^b		14.76 ^c	15.14 ^c	10.94 ^c
	PP							15.37 ^d	16.41 ^e	
	expt.	17.67		23.28		22.41		15.58	15.85	11.76
B	present work	1.25	1.18	1.02	0.96	1.20	1.10	2.87	3.26	1.83
	FP-LMTO	1.14 ^a		1.06 ^a				2.64 ^c	3.29 ^c	1.92 ^c
	PP							2.77 ^d	3.33 ^e	
	expt.	1.10		0.97		1.11		2.65	3.14	1.42
c/a	present work	1.585		1.621		1.580				
	FP-LMTO	1.589 ^a		1.613 ^a		1.594 ^b				
	expt.	1.588		1.592		1.583				

^aReference 30.

^bReference 31.

^cReference 15.

^dReference 16

^eReference 17.

The vacancy computations are performed by the supercell approach,³² using periodically repeated cells, with various numbers of atomic sites N : $N=32$, $N=36$, and $N=27$ and 54 , respectively, for the fcc, hcp, and bcc structures. The vacancy formation energies, E_f , were first calculated at fixed supercell size according to

$$E_f = E(N-1, 1, N\Omega_0) - \frac{N-1}{N} E(N, 0, N\Omega_0), \quad (1)$$

where $E(N-1, 1, N\Omega_0)$ denotes the energy of a supercell with $N-1$ atoms and one vacancy at volume $N\Omega_0$, and $E(N, 0, N\Omega_0)$ is the bulk energy calculated for N atoms at the equilibrium volume. In order to obtain a maximum accuracy, the bulk energies $E(N, 0, N\Omega_0)$ were calculated with a supercell and using the same k points as for the computation of $E(N-1, 1, N\Omega_0)$. These energies were found to differ by less than 2 meV from $NE(1, 0, \Omega_0)$, provided that the same k -point density is used.

We have studied the effect of volume relaxation, by minimizing the energy of the supercell with a vacancy with respect to homogeneous volume changes, leading to a contraction denoted $\Delta\Omega$ and a decrease in energy, ΔE . This allows the calculation of the formation volume, $\Omega_f = \Omega_0 - \Delta\Omega$. The formation enthalpy at constant pressure ($p=0$) is given by $E_f - \Delta E$; its difference with E_f vanishes when $N \rightarrow \infty$ and was found here to be less than 0.04 eV for group-IV elements for $N=27$ and 36 . These relaxation energies are rather small, when compared to the results found in W (Ref. 17) even in relative value, i.e., when normalized to E_f or to the cohesive energy, E_{coh} . This behavior can be partly explained by the fact that ΔE is proportional to $B\Omega_0$ through¹⁰

$$\Delta E \approx \left(\frac{\Delta\Omega}{\Omega_0} \right)^2 \frac{B\Omega_0}{2(N-1)}. \quad (2)$$

$B\Omega_0$ indeed increases by more than a factor of two from group IV to group VI, and $B\Omega_0/E_{\text{coh}}$ increases linearly along the transition metal series. Because ΔE is negligible in group IV, for simplicity the formation energies reported below will always correspond to calculations at constant supercell volume: they will be noted E_f while H_f will be used to represent either results from fully relaxed calculations or experimental values.

III. VALIDATION OF VACANCY CALCULATIONS IN Mo, W, AND Cu

The aim of this section is to assess the reliability of the present procedure, based on the FP-LMTO method, to calculate unrelaxed vacancy energies both in close packed structures and in the bcc structure of transition metals. Going beyond the atomic sphere approximation (ASA) is a prerequisite for such calculations.^{33,14} As shown in the Appendix, the value of the vacancy formation energy calculated with the LMTO-ASA method is indeed too large by almost a factor of 2: we have reproduced this result in Cu and confirmed it through hcp-Zr for the elements of interest in this paper.

The present FP-LMTO results for test calculations of the vacancy formation energy for two elements with the bcc structure (Mo and W) and one with the fcc structure (Cu) are reported in Table II. The result in Cu, 1.35 eV, is in excellent agreement with previous similar FP-LMTO calculations:^{34,15} 1.29 eV and 1.33 eV. The very good agreement with the experimental value of 1.28 eV,⁴ was

TABLE II. Calculated values of the vacancy formation energies in Mo, W, and Cu. The experimental values are recalled in parentheses. The other FP-LMTO results are from Ref. 15, and the pseudopotential (PP) results from Ref. 16 in Mo and from Ref. 17 in W. The calculations are at fixed supercell size and without structural relaxation, except for the last line where fully relaxed results are reported. N is the number of sites and n_k the number of k points. The energies are expressed in eV.

	N	n_k	Mo (2.95 ± 0.25)	W (3.55 ± 0.25)	Cu (1.28 ± 0.05)
Present work	27	16	3.14	3.53	
	54	10	3.16	3.54	
	32	35			1.35
FP-LMTO	27	16	3.13	3.27	
	32	10			1.33
PP	54	4	3.16	3.68	
PP relaxed	54	4	2.90	3.44	

expected since similar agreements were obtained by Korhonen *et al.* within a systematic FP-LMTO study performed over six fcc metals.¹⁵ This demonstrates that, in compact structures: (i) neglecting the structural and volume relaxations and using supercells with 32 atoms or more are very good approximations and (ii) the FP-LMTO method allows to compute reliable vacancy formation energies.

For the bcc structure, Mo and W were chosen because, in addition to experimental data, a large body of information is available for these elements from previous very conclusive DFT-LDA studies using *ab initio* pseudopotentials (PP):^{16,17} the values of the fully-relaxed vacancy formation energies are within the experimental error bars,^{35,36} and the gain in energy due to volume and structural relaxations were found in both cases to be approximately 0.25 eV (see Table II). The FP-LMTO values for the *unrelaxed* vacancy formation energies calculated here for $N=54$ are in perfect agreement with the PP study in Mo, and differ by only 0.14 eV in W (see Table II). This suggests that the implementation of the FP-LMTO method used here is also reliable in the bcc structure for the calculation of *unrelaxed* vacancy formation energies, even though the interstitial region—which is *a priori* treated with less accuracy than the region inside the spheres—is larger than in compact structures. These calculations were repeated with the same supercell size ($N=27$) and number of k points ($n_k=16$) than in the previous similar FP-LMTO study of Ref. 15. The agreement is perfect in Mo, whereas in W the present value is larger by 0.26 eV leading to a significantly better agreement with experiments and PP results. This discrepancy can be attributed either to the fact that a more accurate basis set is used here with four additional Hankel functions—for the s and p orbitals—or to the improved broadening scheme using Hermite Gaussians instead of Gaussians. Besides W, the unrelaxed vacancy formation energies calculated with the FP-LMTO method for 5 other bcc metals in Ref. 15 are found to be slightly to significantly larger than the experimental values. The present implementation which includes the technical improvements mentioned above, as well as the treatment of semicore states, is expected to improve the agreement with the exact DFT-LDA result, which can be one reason for this discrepancy, at least for some elements. But the main reason is most probably the structural relaxation which was shown to be even larger in Ta than in Mo and W.³⁷

As a summary, the present procedure for calculating unrelaxed vacancy formation energies with the FP-LMTO method which was already known to be reliable in compact structures is shown here to be also reliable in the bcc structure with an estimated accuracy for transition metals of 0.2 eV within the DFT-LDA. There is no reason to suspect insufficiencies in the DFT-LDA itself. Therefore the results presented below in group IV, can be considered as reliable predictions for the unrelaxed values of the vacancy formation energies, and the only missing quantities for the direct comparison with the exact values for the real material are the structural-relaxation energies, which will be the object of forthcoming papers.^{38,39}

IV. GROUP-IV RESULTS

A. Formation energies in the hcp structure

The effect of supercell size on the determination of E_f was investigated in hcp-Zr. Cells with $N=16$ are clearly too small to cancel the effect of vacancy-vacancy interactions: the value of E_f is larger by 0.25 eV than for $N=36$. In view of the excellent agreement with experiments obtained for $N=32$ in fcc metals,¹⁵ the results can be considered as converged within approximately 0.1 eV for $N=36$ in the hcp structure. The values of E_f obtained at fixed supercell size for $N=36$ are displayed in Table III.

TABLE III. Vacancy formation energies for group IV elements. The results are reported for constant supercell volume calculations with $N=36$ and $n_k=28$ in the hcp structure and for two different sizes in the bcc structures: $N=27$ and $N=54$ with respectively $n_k=16$ and $n_k=10$. The experimental values are taken from Refs. 40 and 6. In the hcp structure, E_f/Q corresponds to the calculated vacancy formation energy normalized to the experimental value of the activation energy taken from Refs. 2, 3 and 5. The energies are expressed in eV.

		Ti	Zr	Hf
hcp	Calc.	2.14	2.07	2.37
	Expt.		≥ 1.5	2.45 ± 0.2
	E_f/Q	0.68	0.65	0.64
bcc	Calc. $N=27$	2.24	2.34	2.39
	Calc. $N=54$	2.20	2.30	

In Hf the present result, $E_f=2.37$ eV, is in excellent agreement with the experimental determination of the vacancy formation enthalpy in α -Hf,⁶ $H_f^{\text{exp}}=2.45\pm 0.2$ eV, and in Zr ($E_f=2.07$ eV) it is compatible with the experimental evidence from positron annihilation spectroscopy which leads to $H_f^{\text{exp}}\geq 1.5$ eV.⁴⁰ The only *ab initio* data to compare with were obtained using the full potential KKR method in the hypothetical fcc structure of Ti and Zr.⁴¹ The result for Ti in Ref. 41, $E_f=2.13$ eV, is extremely close to the present value ($E_f=2.14$ eV) whereas for Zr the difference between the two values (1.77 eV and 2.07 eV, respectively) is larger than expected for two similar structures. The value predicted by the SMA potential of Ref. 9 for Zr, namely $E_f=2.14$ eV, agrees very well with the present result. The energy decrease due to structural relaxation obtained in the latter study, namely 0.07 eV, suggests that this effect which is not taken into account here is very weak.

The calculated values of E_f in hcp-Ti, hcp-Zr, and hcp-Hf can be considered as quite reliable in view of the general agreement with available experimental and theoretical data discussed above. The results for these three metals are consonant with normal values in the sense they match well with the following correlation stated for metals:^{42,44}

$$H_f=10^{-3}T_m \text{ eV K}^{-1}. \quad (3)$$

The melting temperatures, T_m , of these elements⁴³ indeed lead respectively to $H_f=1.9, 2.1$, and 2.5 eV. Moreover, the ratio between the calculated value of E_f and the experimental values of the self-diffusion activation energy, Q , is remarkably constant for the three elements with a value close to 2/3 (see Table III). This ratio is close to the usual observations in metals.^{40,6} We can therefore conclude that there is a perfect consistency between the present results, the experimental values of Q , and the fact that self diffusion is vacancy controlled with normal defect parameters in the hcp structure of these metals.

B. Formation energies in the bcc structure

The calculations of E_f performed for $N=27$ and $N=54$ in bcc-Ti and bcc-Zr show very weak size effects, namely only 0.04 eV. The calculation was therefore performed only for $N=27$ in bcc-Hf. The results are summarized in Table III. A preliminary LDA PP study with $N=16$ in bcc-Hf yielded a slightly larger value,³⁷ $E_f=2.72$ eV. The size effect probably accounts for part of the difference with the present result ($E_f=2.39$ eV). There are, to our knowledge, no experimental determinations for H_f , and no other *ab initio* data to compare with. Quite surprisingly the present results of E_f are remarkably close to the values obtained in the hcp structure. Since the same absence of crystal-structure effect was obtained from SMA calculations⁹ in Zr ($E_f=2.14$ and 2.10 eV in the hcp and bcc structures, respectively), one can conclude that the electronic structure, even when taken into account at the DFT-LDA level, does not favor the formation of vacancies on a rigid bcc lattice. As a result, the present values are consistent—or even slightly larger than—the normal values expected from Eq. (3). When structural relaxations are not

included, group-IV elements therefore behave as the ten other bcc metals which were shown to follow very well the scaling law of Eq. (3).⁴⁴

The Arrhenius plots of self-diffusion coefficients in bcc-Ti and bcc-Zr are strongly curved,^{45,46} and various values for the activation energies have been proposed depending on the model adopted for the interpretation.⁴⁷ The two energies, Q_1 and Q_2 , deduced from a two-exponential fit, are good indications of slope ranges: in bcc Ti, $Q_1\approx 1.3$ eV and $Q_2\approx 2.5$ eV and in bcc-Zr $Q_1\approx 0.9$ eV and $Q_2\approx 2.1$ eV.⁴⁷ Assuming that the monovacancy mechanism is dominant at low temperatures, the sum of the formation enthalpy, H_f , and the migration enthalpy, H_m , is normally expected to be close to Q_1 at low temperature.⁴⁸ In bcc-Hf, the reduced temperature range allows only a one exponential fit with $Q=1.65$ eV.⁴⁹ The various estimates of the migration enthalpies in bcc-Ti, bcc-Zr, and bcc-Hf (Refs. 9 and 50) indicate small but nonvanishing energies of 0.3–0.4 eV. The unrelaxed vacancy formation energies calculated here are twice or more larger than the difference between Q_1 (or Q) and these estimated migration energies. This discrepancy can be understood within standard diffusion theory only if the structural relaxation energy is very large. The relatively large relaxation found in bcc-Zr with SMA calculations in bcc-Zr, namely 0.57 eV, indeed goes in this direction. The implementation of the FP-LMTO method used here is not very well suited for performing relaxation: the computation of the forces is not accessible and the method has not been tested for such cases. It is therefore more convenient to resort to plane-wave/pseudopotential techniques to investigate this relaxation effect within DFT-LDA.^{38,39}

The large relaxation effect is the only explanation compatible with the vacancy mechanism and standard diffusion theory. Otherwise, if the relaxed vacancy formation energies are normal, the vacancy mechanism is possible only if the migration is anomalous, i.e., for instance if the migration energies are vanishingly small, such as in the omega-embryo model,⁵¹ making invalid application of the transition state theory. The fact that the self-diffusion coefficient increases by three orders of magnitude when going from the hcp-phase to the bcc-phase, is also compatible with these two explanations: either a strong decrease in the activation energy, or a strong difference in the vacancy diffusion due to an anomalously large and temperature dependent prefactor in the bcc structure.

C. Formation volumes

The formation volumes, Ω_f , calculated according to the procedure described in Sec. II—using cells containing $N=36, 27$, and 32 sites, respectively, for the hcp, bcc, and fcc structures—are reported in Table IV for hcp-Ti, bcc-Ti, hcp-Zr, bcc-Zr, hcp-Hf, and Cu. The uncertainty in the determination of Ω_f is rather large, i.e., $\pm 0.1\Omega_0$, because of the difficulty to locate with sufficient accuracy the minimum of energy with respect to volume. An indication of the error on Ω_f is given by the fact that the decrease in energy, ΔE , which is obtained differs by at most 10% from the value expected from Eq. (2). In the interpretation of the present

TABLE IV. Calculated vacancy formation volumes. The gain in energy, ΔE , due to volume relaxation starting from a supercell of volume $N\Omega_0$ is given for $N=36$, 27, and 32, respectively, for the hcp, bcc, and fcc structures.

	hcp-Ti	bcc-Ti	hcp-Zr	bcc-Zr	hcp-Hf	Cu
$\Omega_f(\Omega_0)$	0.60	0.64	0.57	0.70	0.65	0.67
$\Delta E(\text{eV})$	0.03	0.03	0.04	0.02	0.03	0.02

results, one should keep in mind that the effects of long range interactions and of structural relaxations are not taken into account here.

The result in Cu, $\Omega_f=0.67\Omega_0$, is in good agreement with the experimental value of $\Omega_f^{\text{exp}}=0.75\Omega_0$.⁴ The calculated values in the hcp structure are therefore believed to be quite reliable, although the experimental value reported in α -Zr, $\Omega_f^{\text{exp}}=0.95\Omega_0$ ⁴ is substantially larger.

The formation volumes obtained in the bcc structure (0.64 and 0.7 Ω_0) are very similar to the LDA results in other bcc transition metals^{16,17} (0.6 Ω_0 in Mo and 0.62 Ω_0 in W). As for the energies, no significant crystal-structure effect is noticed. The experimental determination of *activation* volumes in group IV yielded much smaller values:^{52,53} $\Omega_a=0.33\Omega_0$ in β -Ti and $\Omega_a\approx 0.2\Omega_0$ in β -Zr. Three explanations are proposed for the large and negative difference, $\Omega_a^{\text{exp}}-\Omega_a^{\text{calc}}$, if a vacancy mechanism is assumed: (i) a strong coupling between structural and volume relaxations; (ii) negative migration volumes: the LDA result in Li (Ref. 54) ($\Omega_m=-0.2\Omega_0$) indeed shows that this is possible; or (iii) strong temperature dependence of Ω_a , which was indeed shown to increase by 0.03 Ω_0 when the temperature is decreased from 1423 K to 1273 K in β -Zr.⁵³ The present results are therefore not incompatible with the experimental determinations of Ω_a , but further investigations are required.

D. Charge distribution

We have analyzed the charge redistribution close to the vacancy. For each site, the charge inside the muffin-tin sphere is compared to the bulk value for the atoms and to zero for the vacancy site. The results are reported in Table V for hcp-Zr and bcc-Zr. The charge redistribution affects only the nearest neighbors of the vacancy: each atom loses 0.05 to 0.06 electron from its muffin-tin sphere. This can be compared to what occurs at metal surfaces, where the same balance yielded a charge transfer of approximately 0.1 electron

TABLE V. Charge redistribution around the vacancy in hcp-Zr and bcc-Zr. The charge balance is performed inside the muffin-tin spheres centered respectively on the vacancy, and a first, second, and third nearest neighbor site. The reference is an empty sphere for the vacancy and a bulk sphere for the atoms. A positive sign indicates an excess of valence electrons.

	hcp-Zr	bcc-Zr
vacancy	0.788	0.671
first neighbor	-0.052	-0.065
second neighbor	0.001	-0.007
third neighbor	-0.015	0.002

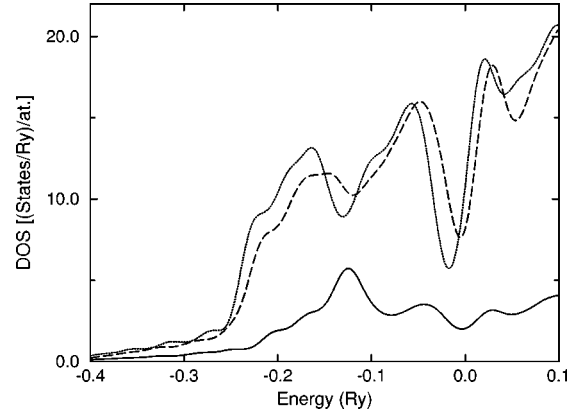


FIG. 2. Local density of states for a bulk atom (dotted line), a first neighbor of the vacancy (dashed line), and the vacancy site (full curve) in hcp-Zr.

per surface atom.⁵⁵ Here, this charge is essentially redistributed on the vacancy site, which in turn has an excess charge of 0.79 and 0.67 electron inside the sphere respectively in hcp-Zr and bcc-Zr. Close to a defect in general, the commonly admitted rule is that of local charge neutrality. The above analysis based on the charge inside the spheres indeed suggest that the atoms far from the vacancy remain neutral, and that the nearest neighbors of the vacancy also conserve their charge, which is partially spread into the empty space left by the vacancy.

The local density of states (DOS) on the nearest neighbor of the vacancy are compared to the bulk DOS: as expected it has a smaller width, and a smoother shape (see Fig. 2). The local DOS obtained by projecting on the vacancy site covers the same energy range and is characteristic of delocalized states.

V. CONCLUSION

It has been shown that the FP-LMTO method provides reliable values for the *unrelaxed* vacancy formation energies, E_f , in bcc transition metals. This result, already admitted for compact structures (fcc and hcp), was obtained by very conclusive comparisons with previous *ab initio* pseudopotential calculations in Mo and W. The values of E_f calculated for group-IV elements (Ti, Zr and Hf), are invariant with crystal structure, hcp or bcc, and are consistent with normal values expected for metals. In the hcp structure, where structural relaxations are believed to be small, this paper provides reliable predictions for H_f in α -Ti and α -Zr, and confirms the experimental value in α -Hf. In the bcc structure, the calculated values of E_f are much larger than the experimental

TABLE VI. Comparison between LMTO-ASA and FP-LMTO methods for the calculation of unrelaxed vacancy formation energies at constant cell volume. The calculations are performed for $N=32$ and $n_k=35$ in Cu (fcc structure), and $N=36$ and $n_k=28$ in hcp-Zr. Energies are expressed in eV.

Method	Cu	hcp-Zr
LMTO ASA	2.32	3.68
FP-LMTO	1.35	2.07

activation energies deduced from the slope of self-diffusion Arrhenius plots. The symmetry of the bcc structure—when the vacancy is introduced on a rigid lattice—is therefore not sufficient to account for the anomalously low values of H_f expected for the vacancy mechanism to be dominant. The alternative explanation which is suggested is therefore a crystal-structure effect entirely due to structural relaxations.^{38,39}

The calculated formation volumes range from 0.57 to 0.70 Ω_0 , without any significant dependence on the crystal structure. The charge redistribution is such that the tail of the charge from the first neighbors of the vacancy extends into the vacancy site, while further neighbors are not affected and remain neutral.

ACKNOWLEDGMENTS

This study was partially supported by the *Direction des Etudes et Recherches of Electricité de France* at Moret-sur-Loing, France, under cooperative CEA-EDF action No.

2337. O.L. and F.W. gratefully acknowledge Dr. M. Methfessel for supplying the FP-LMTO code.

APPENDIX: COMPARISON BETWEEN LMTO-ASA AND FP-LMTO

The LMTO method in the atomic sphere approximation²⁴ (ASA) has a significantly lower computational cost than the FP-LMTO method.¹⁸ However LMTO-ASA calculations including combined correction terms, yield large discrepancies with respect to FP-LMTO. The results of the computations performed under similar conditions using both methods are compared in Table VI for hcp-Zr and Cu. The LMTO-ASA values are larger by almost a factor of 2. There is a minor difference in the set up of the calculations, because the semi-core panel has been included in the FP-LMTO computations but not in the LMTO-ASA case. We checked in hcp-Zr, that the FP-LMTO result is very similar when only one panel is used (E_f is lower by less than 0.01 eV).

- ¹H. Mehrer, N. Stolica, and N.A. Stolwijk, in *Diffusion in Solid Metals and Alloys*, edited by H. Mehrer, Landolt-Börnstein New Series III/26 (Springer, Berlin, 1990), p. 32.
- ²M. Köppers, D. Derdau, M. Friesel, and C. Herzig, *Defect Diffus. Forum* **143-147**, 43 (1997).
- ³G.M. Hood, H. Zou, R. Schultz, N. Matsuura, J.A. Roy, and J. A. Jackman, *Defect Diffus. Forum* **143-147**, 49 (1997).
- ⁴P. Ehrhart, in *Atomic Defects in Metals*, edited by H. Ullmaier, Landolt-Börnstein New Series III/25 (Springer, Berlin, 1991), p. 32.
- ⁵B.E. Davis and W.D. Mc Mullen, *Acta Metall.* **20**, 593 (1972).
- ⁶G.M. Hood and R.J. Schultz, *Mater. Sci. Forum* **175**, 375 (1995).
- ⁷U. Köhler and C. Herzig, *Philos. Mag. A* **58**, 769 (1988).
- ⁸V.G. Kapinos, Y.N. Osetsky, and P.A. Platonov, *J. Nucl. Mater.* **195**, 88 (1992).
- ⁹F. Willaime and C. Massobrio, *Phys. Rev. B* **43**, 11 653 (1991).
- ¹⁰A. De Vita and M.J. Gillan, *J. Phys.: Condens. Matter* **3**, 6225 (1991).
- ¹¹W. Frank, U. Breier, C. Elsässer, and M. Fähnle, *Phys. Rev. B* **48**, 7676 (1993).
- ¹²U. Breier, W. Frank, C. Elsässer, M. Fähnle, and A. Seeger, *Phys. Rev. B* **50**, 5928 (1994).
- ¹³P.H. Dederichs, T. Hoshino, B. Drittler, K. Abraham, and R. Zeller, *Physica B* **172**, 203 (1991).
- ¹⁴B. Drittler, M. Weinert, R. Zeller, and P.H. Dederichs, *Solid State Commun.* **79**, 31 (1991).
- ¹⁵T. Korhonen, M.J. Puska, and R.M. Nieminen, *Phys. Rev. B* **51**, 9526 (1995).
- ¹⁶B. Meyer and M. Fähnle, *Phys. Rev. B* **56**, 13 595 (1997).
- ¹⁷A. Satta, F. Willaime, and S. De Gironcoli, *Phys. Rev. B* **57**, 11184 (1998).
- ¹⁸M. Methfessel, *Phys. Rev. B* **38**, 1537 (1988).
- ¹⁹M. Methfessel, C.O. Rodriguez, and O.K. Andersen, *Phys. Rev. B* **40**, 2009 (1989).
- ²⁰M. Methfessel and M. Scheffler, *Physica B* **172**, 175 (1991).
- ²¹W. Kohn and L.J. Sham, *Phys. Rev.* **140**, A1133 (1965).
- ²²D.M. Ceperley and B.J. Alder, *Phys. Rev. Lett.* **45**, 566 (1980).
- ²³J.P. Perdew and A. Zunger, *Phys. Rev. B* **23**, 5048 (1981).
- ²⁴O.K. Andersen, in *Electronic Structure of Complex Systems*, edited by P. Phariseau and W.M. Temmerman (Plenum, New York, 1984), p. 11.
- ²⁵A.T. Paxton, M. Methfessel, and H.M. Polatoglou, *Phys. Rev. B* **41**, 8127 (1990).
- ²⁶H.J. Monkhorst and J.D. Pack, *Phys. Rev. B* **13**, 5188 (1976).
- ²⁷M. Methfessel and A.T. Paxton, *Phys. Rev. B* **40**, 3616 (1989).
- ²⁸P. Villars and L.D. Calvert, *Pearson's Handbook of Crystallographic Data for Intermetallic Phases* (American Society for Metals, Metals Park, OH, 1985).
- ²⁹G. Simmons and H. Wang, *Single Crystal Elastic Constants and Calculated Aggregate Properties* (MIT, Cambridge, MA, 1971).
- ³⁰V. Ozolins and M. Körling, *Phys. Rev. B* **48**, 18 304 (1993).
- ³¹R. Ahuja, J.M. Wills, B. Johansson, and O. Eriksson, *Phys. Rev. B* **48**, 16 269 (1993).
- ³²M.J. Gillan, *J. Phys.: Condens. Matter* **1**, 689 (1989).
- ³³T. Beuerle, R. Pawellek, C. Elsässer, and M. Fähnle, *J. Phys.: Condens. Matter* **3**, 1957 (1991).
- ³⁴H.M. Polatoglou, M. Methfessel, and M. Scheffler, *Phys. Rev. B* **48**, 1877 (1993).
- ³⁵R. Ziegler and H.E. Schaefer, *Mater. Sci. Forum* **15-18**, 145 (1987).
- ³⁶J.N. Mundy, *Philos. Mag. A* **46**, 345 (1982).
- ³⁷A. Satta, F. Willaime, and S. De Gironcoli, in *Phase Transformations and Systems Driven Far From Equilibrium*, edited by E. Ma, P. Bellon, M. Atzmon, and R. Trivedi, MRS Proceedings No. 481 (Materials Research Society, Pittsburgh, 1998), p. 189.
- ³⁸O. Le Bacq, A. Pasturel, and F. Willaime (unpublished).
- ³⁹F. Willaime, A. Satta, and S. de Gironcoli (unpublished).
- ⁴⁰G.M. Hood, *J. Nucl. Mater.* **139**, 179 (1986).
- ⁴¹B. Drittler, M. Weinert, R. Zeller, and P.H. Dederichs, *Solid State Commun.* **79**, 31 (1991).
- ⁴²C.P. Flynn, *Point Defects and Diffusion* (Clarendon Press, Oxford, 1972), p. 781.
- ⁴³The experimental melting temperatures which are used here correspond to the bcc phase. Some estimates of the hypothetical

- melting temperature of the low temperature hcp phase—to be used for such correlations—have been proposed in α -Ti and α -Zr: N. Matsuura, G.M. Hood, and H. Zou, *J. Nucl. Mater.* **238**, 260 (1996).
- ⁴⁴H. Schultz, *Mater. Sci. Eng., A* **141**, 149 (1991).
- ⁴⁵U. Köhler and C. Herzig, *Phys. Status Solidi B* **144**, 243 (1987).
- ⁴⁶C. Herzig and H. Eckeler, *Z. Metallkd.* **70**, 215 (1979).
- ⁴⁷G. Neuman and V. Tölle, *Philos. Mag. A* **61**, 563 (1990).
- ⁴⁸The curvature can then be interpreted as due either to the temperature dependence of the vacancy parameters or to a second diffusion mechanism.
- ⁴⁹C. Herzig, L. Manke, and W. Bussmann, in *Point Defects and Defect Interaction in Metals*, edited by J.I. Takamura, M. Doyama, and M. Kiritani (University of Tokyo, Tokyo, 1982), p. 578.
- ⁵⁰H.R. Schober, W. Petry, and J. Trampenau, *Phys. Chem. Liq.* **4**, 9321 (1992).
- ⁵¹J.M. Sanchez and D. de Fontaine, *Phys. Rev. Lett.* **35**, 227 (1975).
- ⁵²R. Jeffery, *Phys. Rev. B* **3**, 4044 (1971).
- ⁵³P. Knorr, J. Jun, W. Lojkowski, and C. Herzig, *Phys. Rev. B* **57**, 334 (1998).
- ⁵⁴U. Breier, V. Schott, and M. Fähnle, *Phys. Rev. B* **55**, 5772 (1997).
- ⁵⁵S. Sawaya, J. Goniakowski, C. Mottet, A. Saúl, and G. Tréglia, *Phys. Rev. B* **56**, 12 161 (1997).